Arch Appl Mech (2009) 79: 741–751
DOI 10.1007/s00419-008-0250-5

ORIGINAL

Abdullah H. M. AlEssa

One-dimensional finite element heat transfer solution of a fin with triangular perforations of bases parallel and towered its base

Received: 25 October 2007 / Accepted: 17 June 2008 / Published online: 4 July 2008

Abstract Heat transfer dissipation from a horizontal rectangular fin embedded with equilateral triangular perforations is computed numerically using one-dimensional finite element technique. The bases of the triangles are parallel and toward the fin base. The body of the fin is discretized into a number of subdivisions (finite elements). The number of these elements can be altered as required according to the automatic mesh generation. The heat dissipation of the perforated fin is computed and compared with that of the solid one of the same dimensions and same thermal properties. The comparison refers to acceptable results and heat dissipation enhancement due to certain perforation.

Keywords Finite element · Perforated fin · Heat dissipation · Heat transfer enhancement

List of symbols

A	cross sectional area of the solid fin (m^2)
A_c	cross sectional area of the triangle perforation (m^2)
A_e	cross sectional area of the finite element (m^2)
A_{pc}	area of the inner surface of the perforation (m^2)
A_{ps}	area of the perforated surface of the fin (m^2)
b	triangle perforation dimension (m)
h	heat transfer coefficient ($W/m^2°C$)
h_{pc}	heat transfer coefficient of the inner surface of the perforation ($W/m^2°C$)
h_{ps}	heat transfer coefficient of the perforated surface of the fin (W/m^2 °C)
h_s	heat transfer coefficient of surface of the two sides of the fin (W/m^2 °C)
h_t	heat transfer coefficient of the fin tip (W/m^2 °C)
k	thermal conductivity of fin material (W/m °C)
L	fin length (m)
l	vector unit (m)
Le	finite element length (m)
N	number of perforations
P	fin perimeter (m)
Pe	finite element perimeter (m)

A. H. M. AlEssa (✉)
Mechanical Engineering Department, Al-Huson University College, Al-Balqa Applied University,
Al-Huson-Irbid, P. O. Box 50, Salt, Jordan
E-mail: abdd104@yahoo.com
Tel.: +962-2-7020483
Fax: +962-2-7010398

Q	fin heat dissipation rate (W)
RQF	ratio of heat dissipation rate of perforated fin to that of non-perforated (solid) one
S	perforation spacing (m)
t	fin thickness (m)
Ve	finite element volume (m^3)
W	fin width (m)

Subscripts and superscripts

b	fin base
e	finite element
max	maximum
pf	perforated fin
pc	inner surface of the perforation (lining surface of the perforation)
ps	perforated surface which is the remaining solid portion of the perforated fin
s	solid surfaces of the fin sides
sf	solid (non-perforated) fin
t	fin tip
x	in or along the direction of x-axis
y	in or along the direction of y-axis
z	in or along the direction of z-axis
∞	ambient

1 Introduction

Compact heat exchangers are designed in configurations that have a large heat transfer surface area per unit of volume. The large area per unit of volume can be attained by attaching extended surfaces (fins). The fins of the plate-fin surfaces are frequently cut into segments or otherwise interrupted in various ways. These modifications are for increasing the heat transfer coefficient and sometimes to increase heat transfer surface area [1,2]. It is worth mentioning that a large number of studies have been conducted to find the optimum shape of fins (rectangular, triangular, pin, wavy, serrated, and slotted). Some of these studies are based on splitting a certain dimension of the fin in an optimal way provided that the total volume of the fin material is fixed. Others have introduced some shape modifications by cutting some material from the fin to make cavities, holes, slots, grooves, or perforations through the fin body [2–5]. Due to the high demand for lightweight, compact, and economical fins, the optimization of fin size is of great importance [6]. Therefore, fins must be designed to achieve maximum heat removal with minimum material expenditure taking into account, however, the ease of manufacturing of the fin shape. One popular heat transfer augmentation technique involves the use of rough surfaces of different configurations. The surface roughness aims at promoting surface turbulence that is intended mainly to increase the heat transfer coefficient rather than the surface area [1]. Several other researchers reported a similar trend for interrupted (e.g., perforated) fins attributing the improvement to the restarting of the thermal boundary layer after each interruption indicating that the increase in convection coefficient is more than enough to offset lost area, if there is any [2,6,7]. The fin industry has been engaged in continuous research to reduce the fin size, weight and cost. The reduction in fin size and cost is achieved by the enhancement of heat transfer carried out by the fins. This enhancement can be accomplished by the following means:

1. Increasing the ratio of the heat transfer surface area of the fin to its volume.
2. Manufacturing fins from materials having high thermal conductivity.
3. Increasing the heat transfer coefficient between the fin and its surroundings.

Perforated plates or perforated fins represent an example of surface interruption [3]. They are widely used for multiple-plate heat exchangers, film cooling (e.g., of turbine blades), and solar collector applications [8]. This study aims mainly to solve the problem of heat transfer from a fin with triangular surface perforations.

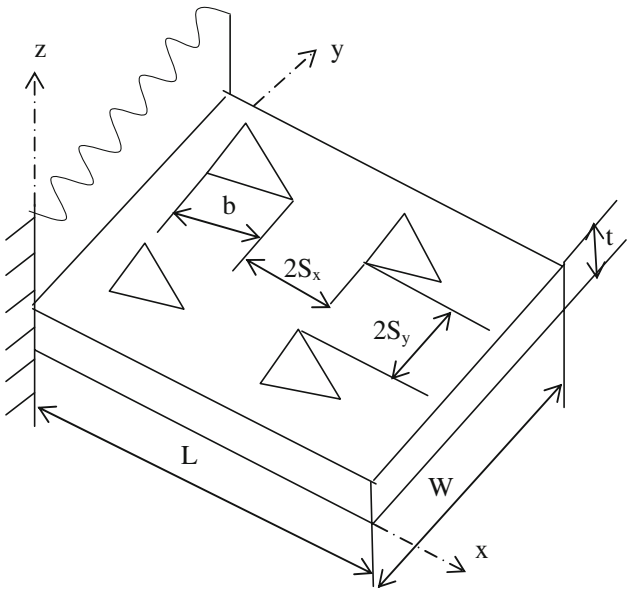

Fig. 1 The fin with equilateral triangular perforations

2 Assumption for analysis

The study of most heat transfer references shows that the classical analyses of fins employ a one-dimensional heat conduction model. The Biot number is very small (less than 0.01), therefore a one-dimensional solution can be considered [9,10]. The analysis and results reported in this study are based on the following assumptions:

1. Steady-state, one-dimensional analysis.
2. The fin material is homogeneous and isotropic with constant thermal conductivity.
3. No heat sources/sinks in the fin body.
4. Uniform base and ambient temperatures.
5. The surface heat transfer coefficients are uniform.

3 Heat transfer analysis

The perforated fin with triangular perforations which is considered in this study is shown in Fig. 1. Figure 2 shows the symmetry part considered for heat transfer analysis (shown hatched). For this part the transverse Biot number in or along the direction of z-axis (Bi_z) can be calculated by $(Bi_z = h_{\mathrm{pc}}t/2k)$ and the transverse Biot number in or along the direction of y-axis (Bi_y) can be calculated by $\left(Bi_y = h_{\mathrm{ps}}(S_y + b/2)/k\right)$. Since the values of (Bi_z) and (Bi_y) are less than 0.01, the heat transfer in (z) and (y) directions can be assumed lumped and a one-dimensional solution can be considered. If the values of (Bi_z) and (Bi_y) are greater than 0.01, then the heat transfer solution must be two or three dimensions. In this study the parameters of the perforated fin are taken as they lead to values of (Bi_z) and (Bi_y) smaller than 0.01. Based on the above assumptions, the energy equation of the fin along with the boundary conditions and according to Figs. 1, 2 and 3 may be stated as below [11]

$$k\frac{\mathrm{d}^2T}{\mathrm{d}x^2} = 0 \tag{1}$$

The associated boundary conditions are

1. At the base surface (x =0)

$$T = T_b \tag{2}$$

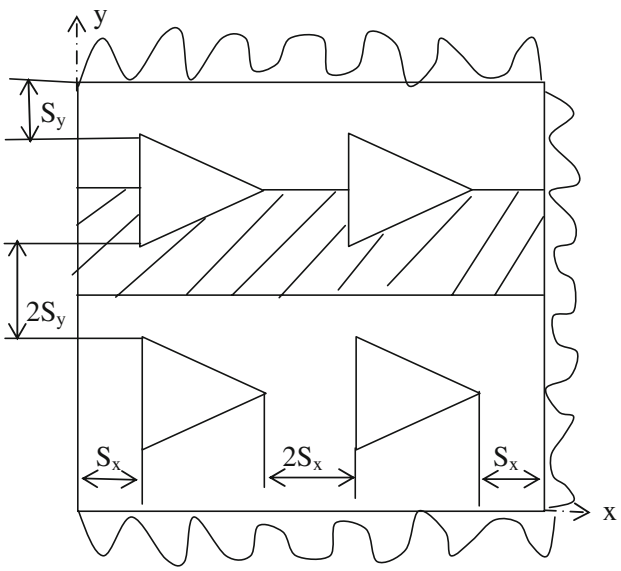

Fig. 2 The symmetrical hatched part used in the mathematical formulation of the perforated fin

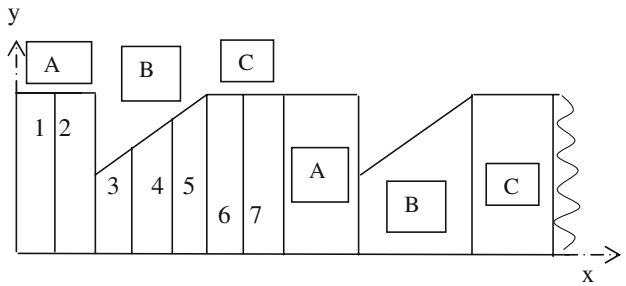

Fig. 3 Expanded symmetrical part with the three regions A, B and C considered in the mathematical formulation (1, 2, 3,. . .. Numbers of the linear finite elements)

2. At the perforated surfaces and the tip of the fin

$$kA_e\frac{dT}{dx}l_x + h_{ps}A_{ps}(T - T_\infty) + h_{pc}A_{pc}(T - T_\infty) + h_tA_t(T_t - T_\infty) = 0 \tag{3}$$

In this study, the energy equation shown in (1) is solved numerically utilizing the one dimensional finite-element technique. The corresponding variational statement as it is described in [11] has the following form:

$$I_n = \frac{1}{2}\iiint_{Ve} k\left(\frac{dT}{dx}\right)^2 dV + \frac{1}{2}\iint_{A_{ps}} h_{ps}(T - T_\infty)^2 dA_{ps} + \frac{1}{2}\iint_{A_{pc}} h_{pc}(T - T_\infty)^2 dA_{pc} + \iint_{A_t} h_t(T_t - T_\infty)T\, dA_t \tag{4}$$

The variational approach in matrix notation [11] is used in formulating the algebraic equations of the problem of this perforated fin. The formulation of these equations can be found in detail in [11]. The perforated fin elements and body discretization of the symmetry part are shown in Figs. 2 and 3. As shown in Fig. 3, surrounding each semi-perforation there are three regions labeled A, B, and C. These regions which repeat themselves along x direction around each perforation are considered in formulating the discretization mesh and finite element equations. The regions A and C are divided into N_f elements each, while the region B

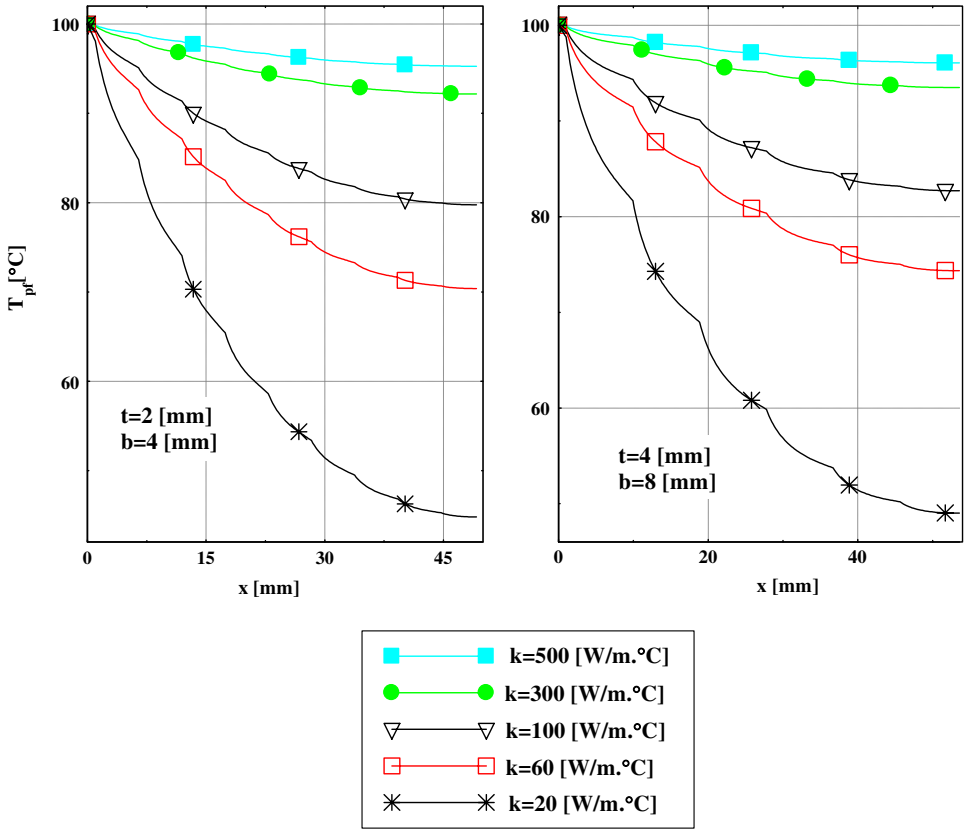

Fig. 4 Temperature distribution of the perforated fin along its length

is divided into N_t elements each. The perforated fin length and width can be computed by the following equations:

$$L = N_x(2S_x + b\text{Sin}\,(60^\circ)) \tag{5}$$
$$W = N_y(2S_y + b) \tag{6}$$

To compare the perforated fin with the solid one, their dimensions (length, width, and thickness) are considered the same. The solid and perforated fin heat transfer surfaces can be computed by the following equations:

$$A_{\text{sf}} = PL + Wt \tag{7}$$
$$\begin{aligned} A_{\text{pf}} &= A_{\text{sf}} + N_x N_y (A_{\text{pc}} - 2A_c) \\ &= A_{\text{sf}} + N_x N_y (3bt - b^2\text{Sin}(60^\circ)) \end{aligned} \tag{8}$$

The total number of elements N_e and the total number of nodes N_n are expressed as:

$$N_e = N_x(2N_f + N_t) \tag{9}$$
$$N_n = N_e + 1 \tag{10}$$

The results of this solution are the perforated fin temperature distribution along its length direction (x coordinate). Once the temperature distribution along the perforated fin length is obtained, the heat dissipation rate from the perforated fin (Q_{pf}) can be computed by one of the following three expressions:

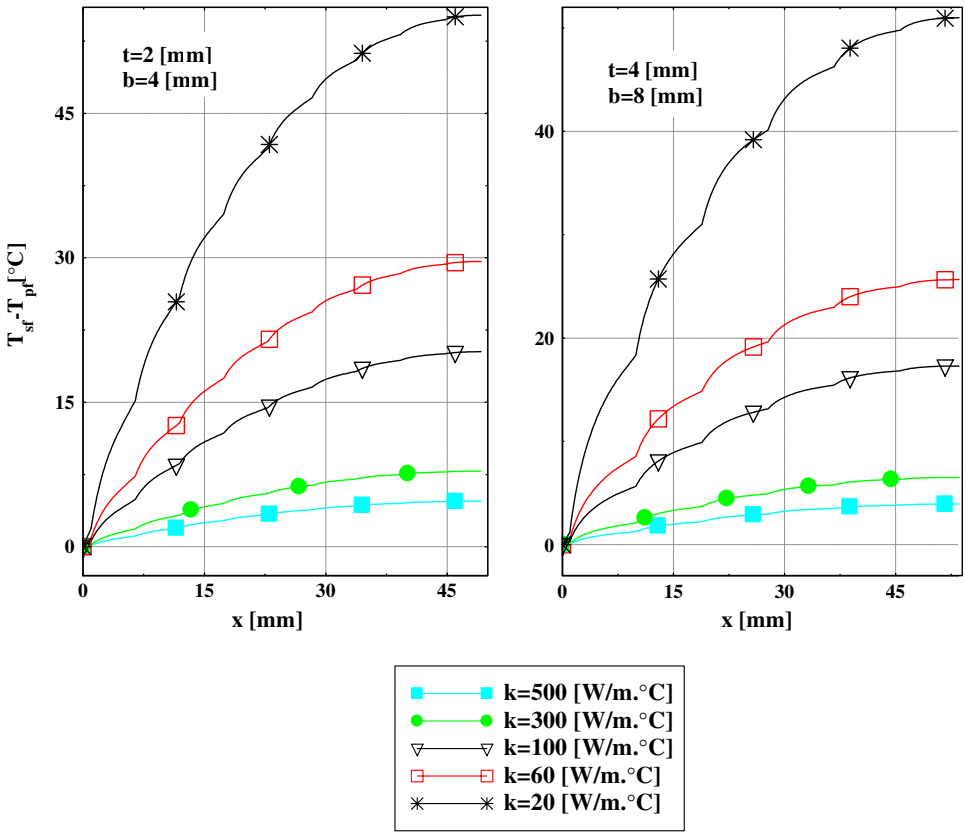

Fig. 5 Temperature difference between that of the solid fin and that of the perforated one along its length

1. The expression of heat dissipation that depends on the integration over all the perforated fin surfaces which can be converted into summation over all finite elements as shown here:

$$Q1 = 2N_y \sum_{I=1}^{N_e} \left(\frac{T_I + T_{I+1}}{2} - T_\infty \right) \left(h_{\mathrm{ps}} \left(\frac{\mathrm{Pe}(I) + \mathrm{Pe}(I+1)}{2} \right) \mathrm{Le}(I) h_{\mathrm{pc}} L_{\mathrm{pc}}(I) t \right) + Q_{\mathrm{t}} + Q_{\mathrm{s}} \tag{11}$$

where Q_{t} and Q_s are the heat dissipation from the tip and the two sides of the perforated fin, and can be calculated by the following expressions:

$$Q_t = A_t h_t (T_t - T_\infty) \tag{12}$$

$$Q_s = 2 \sum_{I=1}^{N_e} \left(\frac{T_I + T_{I+1}}{2} - T_\infty \right) (h_s \mathrm{Le}(I) t) \tag{13}$$

2. The expression of heat dissipation that depends on Fourier's Law:

$$Q2 = -kA \left(\frac{\mathrm{d}T}{\mathrm{d}x} \right)_{at\ x=0} = -2N_y kt \left(S_y + b/2 \right) \left(\frac{\mathrm{d}T}{\mathrm{d}x} \right)_{at\ x=0} \tag{14}$$

The first derivative of the temperature distribution at $(x = 0)$ can be approximated by using the two temperatures of the two nodes of the first finite element of the fin as shown in the following expression:

$$Q2 = 2N_y kt (S_y + b/2) \frac{T_1 - T_2}{Le} \tag{15}$$

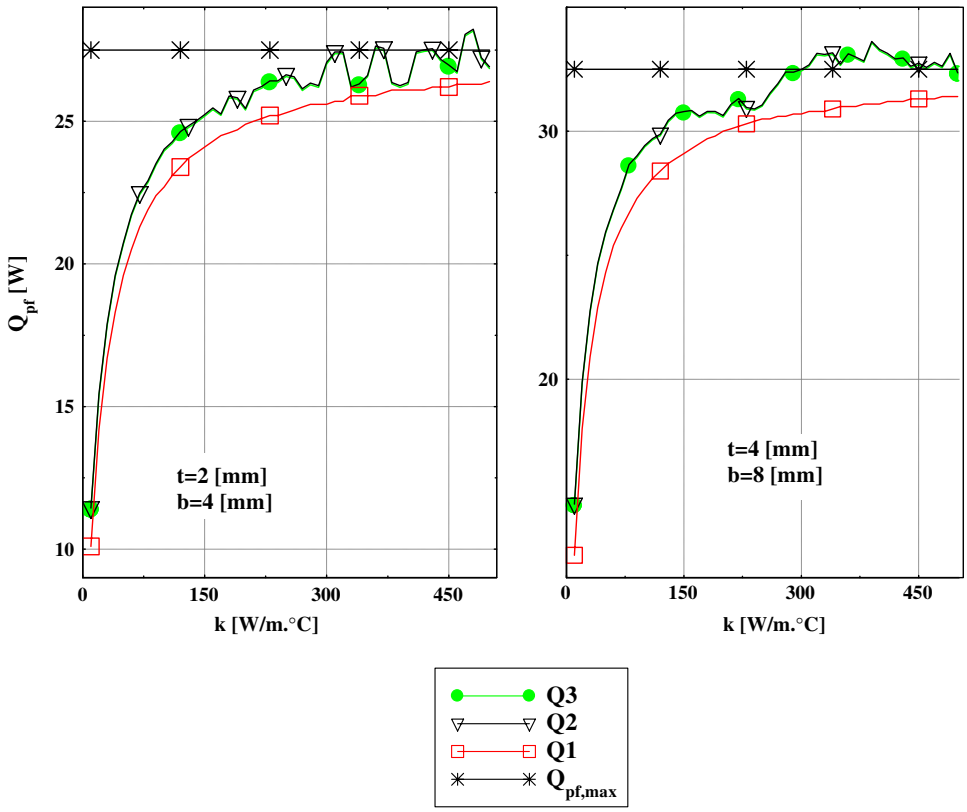

Fig. 6 Heat dissipation rate of the perforated fin as a function of its thermal conductivity for various triangular perforation dimensions

3. The expression of heat dissipation that depends on the first equation of the algebraic equation system which can be expressed as:

$$Q3 = 2N_y(\mathrm{GK}(1,1)T_1 + \mathrm{GK}(1,2)T_2) \tag{16}$$

where GK(1,1) and GK(1,2) are the first and second constants of the first algebraic equation in the finite element solution.
The theoretical maximum heat dissipation of the fin is obtained when the temperature of the whole fin body equals the fin base temperature and it can be computed by the following expression:

$$Q_{\mathrm{pf,max}} = (A_{\mathrm{ps}}h_{\mathrm{ps}} + N_x N_y A_{\mathrm{pc}}h_{\mathrm{pc}} + A_{\mathrm{t}}h_{\mathrm{t}} + A_{\mathrm{s}}h_{\mathrm{s}})(T_b - T_\infty) \tag{17}$$

The fin efficiency is defined as the ratio of the heat transfer from the fin in its actual temperature distribution to its maximum heat transfer. Consequently, the fin efficiency is expressed as

$$\eta_{\mathrm{pf}} = Q_{\mathrm{pf}}/Q_{\mathrm{pf,max}} \tag{18}$$

In order to compare performance of the perforated fin with that of the solid (non-perforated) one of the same dimensions, the equations of the solid fin consider convection heat transfer from its tip as described in case A, Table 3.4, p. 118 of the Ref. [12] are used. The ratio of the heat dissipation of the perforated fin to that of the solid one (RQF) is introduced and given by:

$$\mathrm{RQF} = Q_{\mathrm{pf}}/Q_{\mathrm{sf}} \tag{19}$$

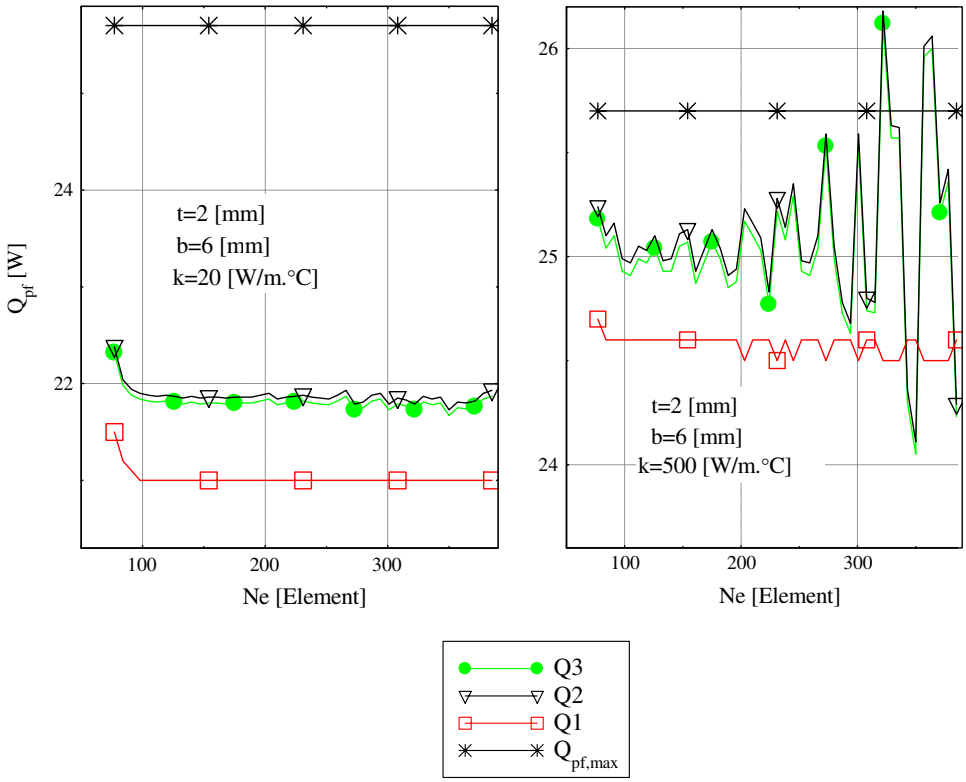

Fig. 7 Fin dissipation rate as a function of the finite element number of the perforated fin

4 Result and discussion

It is believed that comparing the perforated fin with its solid counterpart is the best means to evaluate the difference in heat transfer brought about by introducing the fin perforations. In the following analysis, verification, and discussion, and where there is a comparison between the two fins, it is assumed that both fins have the same dimensions ($L = 50$, $W = 100$ mm), same thermal conductivity, same heat transfer coefficient for all surfaces of the perforated and solid fins ($h = h_{pc} = h_{ps} = h_s = h_t$), and same base temperature ($T_b = 100°C$) and ambient temperature ($T_\infty = 20°C$). The other values are mentioned in their suitable places.

4.1 Temperature distribution of the perforated fin

The temperature distribution along the fin length has an important effect on the fin's performance. Higher fin temperatures can be obtained as the fin's thermal conduction resistance is decreased. The temperature distribution of the perforated fin (T_{pf}) along the x-coordinate is plotted in Fig. 4. From the figure it is obvious that the temperature distributions show non uniform curves caused by perforations which lead to varying area of cross sections along the fin's length and then lead to varying thermal resistance in the fin. The effect of variation of cross sectional area of the perforated fin on thermal resistance decreases as the thermal conductivity increases so the curves become more uniform. To compare the temperature distribution of the perforated fin with that of the solid one, the temperature difference distribution of the solid fin and the perforated fin ($T_{sf} - T_{pf}$) is plotted in Fig. 5. As shown in the figure it is obvious that the temperatures along the solid fin are higher than those of the perforated one in all cases. This is because the thermal conduction resistance of the perforated fin is always higher than that of the corresponding non-perforated one. As the thermal conductivity increases the difference ($T_{sf} - T_{pf}$) decreases and it approaches zero as the thermal conductivity approaches infinity. That is, because as thermal conductivity approaches infinity then the fin (solid or perforated) becomes isothermal with the base temperature (T_b). Figures 4 and 5 show that the temperature difference (temperature drop) between

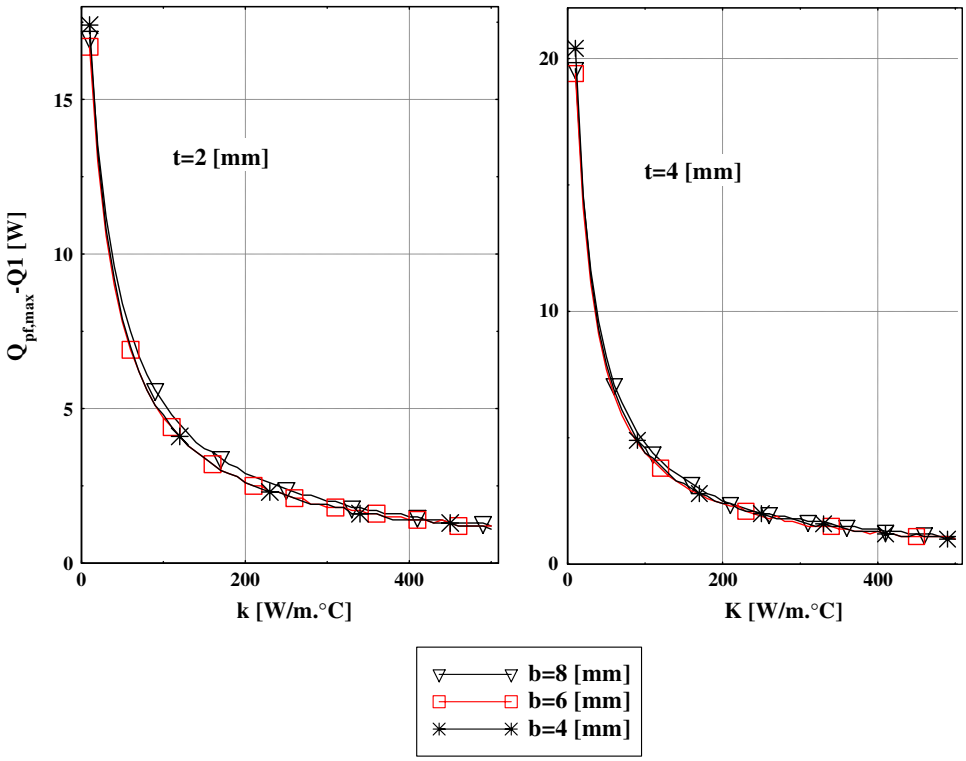

Fig. 8 Fin dissipation rate difference between the maximum value and the actual one of the perforated fin as a function of the thermal conductivity

the fin base and its tip increases as the triangular perforation dimension (b) is increased. This is because the thermal resistance of the perforated fin increases as (b) is increased. Consequently, from only a temperature distribution viewpoint, it would be recommended to use a perforation with dimensions as small as possible. Also it can be deduced from temperature distribution that fin temperatures increase as the fin thickness is increased. This is readily explained by the fact that the thermal resistance of the perforated fin decreases as the fin thickness is increased. Therefore, from the temperature distribution viewpoint, it is preferable to use as large as possible fin thickness. The temperature and temperature difference distributions shown in Figs. 4 and 5 indicate acceptable results as they are compared with those of the solid fin.

4.2 Heat dissipation rate of the perforated fin

The heat dissipation rates ($Q1$, $Q2$, $Q3$ and $Q_{\mathrm{pf,max}}$) of the perforated fin are plotted in terms of fin thermal conductivity with various triangular perforation dimension (b) and fin thickness as shown in Fig. 6. The results show that *Q1* differs from the values of *Q2, Q3*. The value of Q1 seems acceptable because it does not exceed the maximum value ($Q_{\mathrm{pf,max}}$). The values of *Q2* and *Q3* seem unacceptable because they fluctuate around and exceed the maximum value ($Q_{\mathrm{pf,max}}$). The reason for wrong values of *Q2* and *Q3* is that these values are computed by Eqs. (15, 16) in which the calculations depend on the temperatures (T_1 and T_2) at the two sides of the first finite element. This means that any error in (T_1 and T_2) will be significantly reflected on the values of *Q2, Q3*. The value *Q1* depends on all temperatures $T_1, T_2, T_3, \ldots, T_n$ of the finite elements. This means that the errors in the finite element temperatures will diminish one another. To check the stability and convergence of the perforated fin heat dissipations (*Q1, Q2, Q3*) according to the finite element number in the discretization mesh, they are plotted as a function of (N_e) in Fig. 7. Again *Q1* gives good stability and convergence, while *Q2* and *Q3* fluctuate irregularly below or around the ($Q_{\mathrm{pf,max}}$). From the previous results the perforated fin's heat dissipation computed according to the integration overall the fin heat transfer surface *Q1* is more accurate and acceptable. So, it will be adapted in the following calculation.

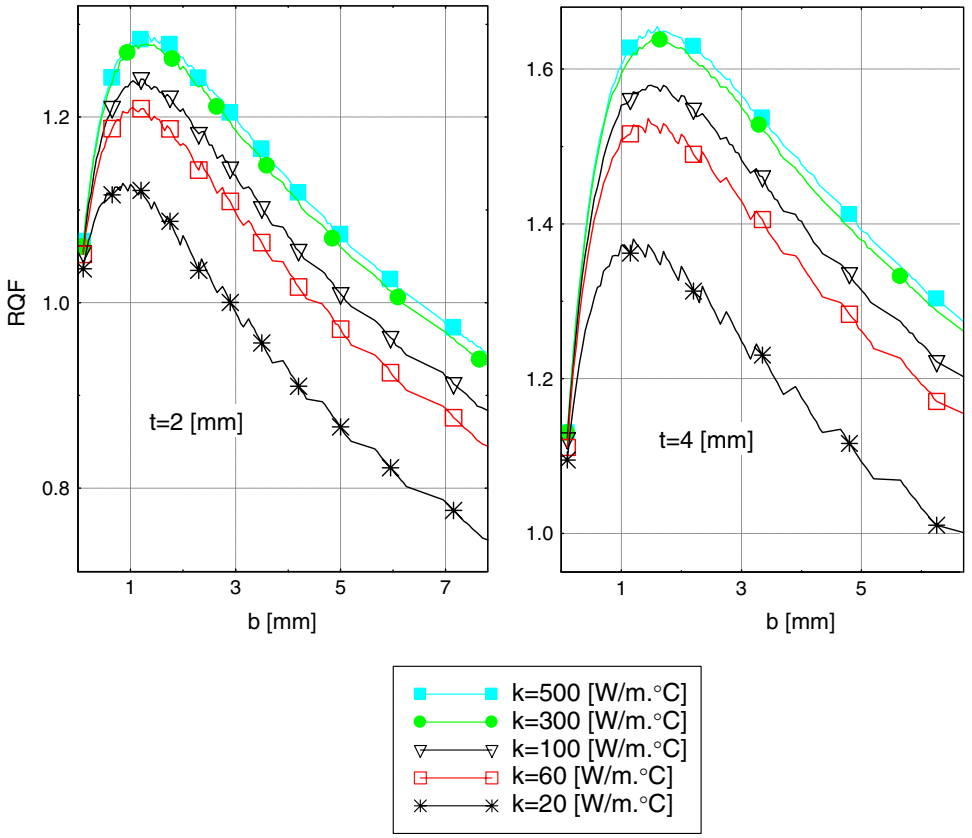

Fig. 9 Heat dissipation ratio of the perforated fin to that of the non perforated one as a function of the triangular perforation dimension

4.3 Verification of the perforated fin heat dissipation rate (Q1)

For more verification of $Q1$, the difference $(Q_{\mathrm{pf,max}} - Q1)$ as a function of fin thermal conductivity for various fin thicknesses and perforation dimensions is plotted in Fig. 8. The theoretical knowledge of the fin analysis implies a positive difference of $(Q_{\mathrm{pf,max}} - Q1)$ and it converges to zero as the fin thermal conductivity approaches very high values. The results in Fig. 8 are consistent with the theoretical knowledge mentioned above. To compare the perforated fin heat dissipation rate with that of the solid one, RQF is plotted as a function of perforation dimension as shown in Fig. 9. It is theoretically expected that RQF should converge to (RQF = 1) as the perforation dimension approaches very small values. This situation is easily observed in Fig. 9. From Fig. 9 it can be deduced that the perforations for certain values of perforation dimension lead to heat transfer enhancement. This means that the use of perforation with certain values of perforation dimension leads to heat transfer enhancement, while the other values lead to heat transfer retardation.

4.4 Perforated fin efficiency (η_{pf})

The perforated fin efficiency according to the value of $(Q1)$ is plotted in Fig. 10. The efficiency has uniform curves with very small wiggles that converge to 100% as the fin's thermal conductivity approaches very high values. This result seems correct and acceptable.

5 Conclusions

1. The one-dimensional heat transfer solution of the perforated fin leads to acceptable results as the Biot Number in lateral directions less than 0.01.

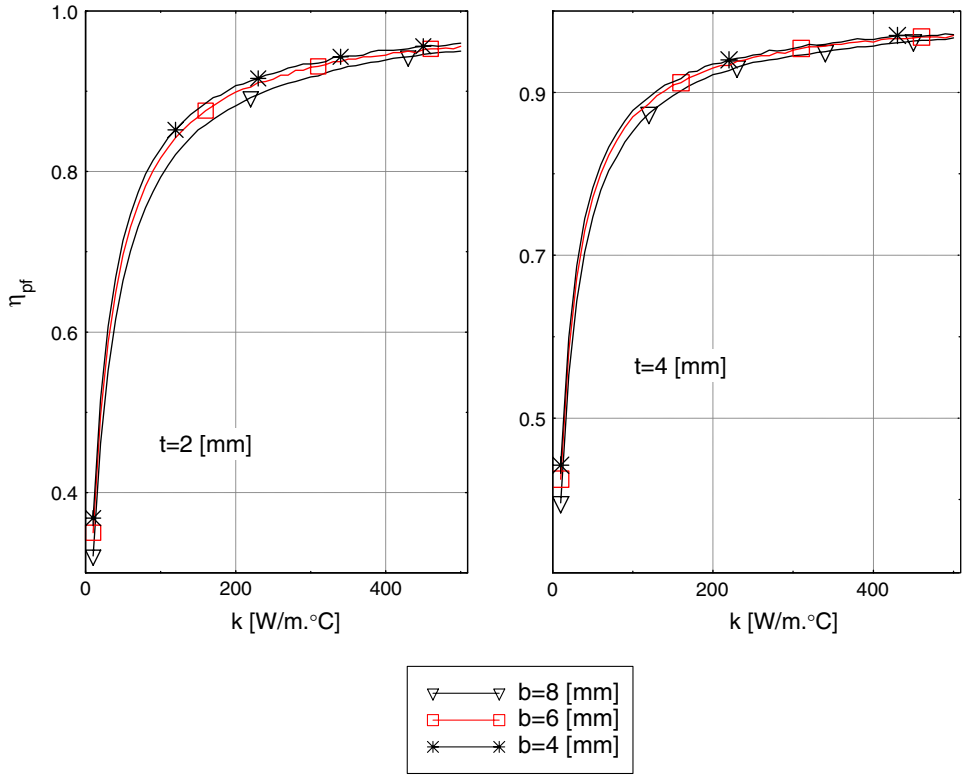

Fig. 10 Perforated fin efficiency as a function of its thermal conductivity for various fin thicknesses and triangular perforation dimensions

2. The geometric modification made by perforation improves the performance of the fin for certain perforation dimensions.
3. The effect of thermal conduction resistance of the fin due to perforation can be decreased as its thermal conductivity is increased.

References

1. Bergles, A.E.: Technique to augment heat transfer. In Handbook of heat transfer Applications. In: Rohsenow W.M., Hartnett J.P., Ganic E.N. (eds.), Chap. 3, 2nd edn. McGraw-Hill Book company, New York (1985)
2. Shah, R.K.: Classification of heat exchangers. In: Kakac, S., Bergles, A., Mayinger, F. (eds.) Heat Exchangers, Thermal-Hydraulic Fundamentals and Design. Hemisphere Publishing, New York (1981)
3. Mullisen, R., Loehrke, R.: A study of flow mechanisms responsible for heat transfer enhancement in interrupted-plate heat exchangers. J. Heat Transfer (Trans. ASME) **108**, 377–385 (1986)
4. Prasad, B.V.S.S.S., Gupta, A.V.S.S.K.S.: Note on the performance of an optimal straight rectangular fin with a semicircular cut at the tip. Heat transfer Eng. vol. 14, no. 1 (1998)
5. Al-Essa, A.H.: Enhancement of thermal performance of fins subjected to natural convection through body perforation. PhD Thesis, Department of Mechanical Engineering, University of Baghdad, Iraq and Jordan University of Science and Technology (2000)
6. Sparrow, E.M., Carranco Oritz, M.: Heat transfer coefficient for the upstream face of a perforated plate positioned normal to an oncoming flow. Int. J. Heat Mass Transfer **25**(1), 127–135 (1982)
7. Al-Essa, A.H., Al-Hussien, F.M.S.: The effect of orientation of square perforations on the heat transfer enhancement from a fin subjected to natural convection. Heat Mass Transfer **40**, 509–515 (2004)
8. Kutscher, C.F.: Heat exchange effectiveness and pressure drop for air flow through perforated plates with and without crosswind. J. Heat Transfer **116**, 391–399 (1994)
9. Razelos, P., Georgiou, E.: Two-Dimensional effects and design criteria for convective extended surfaces. Heat Transfer Eng. **13**(3), 38–48 (1992)
10. Aziz, A., Lunadini, V.: Multidimensional steady conduction in convicting, radiating, and convicting-radiating fins and fin assemblies. Heat Transfer Eng. **16**(1), 32–64 (1995)
11. Rao, S.S.: The Finite Element Method in Engineering, 2nd edn. Pergamon, Elmsford (1989)
12. Incropera, F.P., Dewitt, D.P.: Fundamentals of Heat and Mass Transfer, 4th edn. Wiley, New York (1996)